Aalborg Universitet

AALBORG UNIVERSITY

Breaking the Transmitter-Receiver Isolation Barrier in Mobile Handsets with Spatial Duplexing

Alrabadi, Osama; Tatomirescu, Alexandru; Knudsen, Mikael; Pelosi, Mauro; Pedersen, Gert Frølund

Published in:
I E E E Transactions on Antennas and Propagation

DOI (link to publication from Publisher):
10.1109/TAP.2012.2232897

Publication date:
2013

Document Version
Early version, also known as pre-print

Link to publication from Aalborg University

Citation for published version (APA):
Alrabadi, O., Tatomirescu, A., Knudsen, M., Pelosi, M., & Pedersen, G. F. (2013). Breaking the Transmitter-Receiver Isolation Barrier in Mobile Handsets with Spatial Duplexing. *I E E E Transactions on Antennas and Propagation*, *61*(4), 2241 - 2251. https://doi.org/10.1109/TAP.2012.2232897

General rights
Copyright and moral rights for the publications made accessible in the public portal are retained by the authors and/or other copyright owners and it is a condition of accessing publications that users recognise and abide by the legal requirements associated with these rights.

- Users may download and print one copy of any publication from the public portal for the purpose of private study or research.
- You may not further distribute the material or use it for any profit-making activity or commercial gain
- You may freely distribute the URL identifying the publication in the public portal -

Take down policy
If you believe that this document breaches copyright please contact us at vbn@aub.aau.dk providing details, and we will remove access to the work immediately and investigate your claim.

Downloaded from vbn.aau.dk on: May 02, 2026

Breaking the Transmitter-Receiver Isolation Barrier in Mobile Handsets with Spatial Duplexing

Osama N. Alrabadi[1], Alexandru D. Tatomirescu[1], Mikael B. Knudsen[2], Mauro Pelosi[1] and Gert F. Pedersen[1]

***Abstract*—In full-duplex radio communication systems like e-UTRAN, CDMA-2000, the radio transmitter (Tx) is active at the same time as the radio receiver (Rx). The Tx and the Rx will be using separate dedicated frequency bands and the Tx-Rx isolation is ensured by duplex filters. However, agile duplexers required for multiband operation are almost non-existent while dedicating a bank of narrowband filters is bulky and incurs considerable switching losses. In this article we propose an approach that dramatically reduces the complexity of the RF frontend, first by replacing the duplex filter with a spatial filter and second, by co-designing the filtering antennas and the RF frontend. The spatial filter is synthesized by equipping the Tx with redundant antennas. By properly weighting the Tx antennas, the Tx signal is selectively attenuated in the Rx direction. The spatial filter can be tuned to different frequency bands as long as the antennas are made tunable. Moreover, the spatial filter may directly benefit from the balanced architecture of the power amplifiers (PAs) thus reducing the total system complexity and insertion loss. Finally, simulation and initial measurement results are provided in a challenging low-frequency band, serving as a proof-of-concept.**

***Index Terms*—Duplexing, Decoupling, Null-steering, Spatial filter, Transmitter-receiver isolation, Zero-forcing.**

I. Introduction

CURRENT and future mobile handsets need to accommodate an increasing number of frequency bands and to cope with sophisticated wireless standards like the Advanced Long Term Evolution (LTE-A) for supporting higher data rates. At the same time, handheld terminals have to stay efficient, performance reliable and cost affordable. The miniaturization trend in the handset form factor together with the large frequency spectrum to be covered by the antenna system (700 to 2600 MHz and later up to 3600 MHz) results in many design challenges in the antenna system design besides complicating the transceiver Radio Frequency (RF) frontend architecture. Moreover, ignoring the time-varying disturbance incurred by the user head and hand on the wireless antenna system leads to a significant number of call drops [1], limiting the overall system performance. The co-design of the RF frontend and the antenna system is a promising approach that can solve some the aforementioned design challenges. In such an approach, the antenna needs to provide some functionalities different from the conventional functionality of acting as a mere electromagnetic radiator, e.g. RF filtering [2]. Moreover, some RF components can be modified to provide dual or multiple functionalities while redundant RF components can be removed, thus reducing cost, size and losses. An example of such joint optimization is the co-design of the antenna and the power amplifier (PA) circuit. For example, [3] suggests to directly connect the differential feed of a balanced antenna to the output of a balanced PA, thus the antenna is employed as an out-of-phase spatial combiner. Such architecture dispenses with using baluns or hybrid couplers for converting the balanced PA output into single ended. The architecture results in almost zero insertion loss and higher PA efficiency while the use of balanced antennas immunizes (to some level) the mobile handset against the user proximity effect [4]. Besides PA efficiency and immunity to user proximity effects, Tx-Rx isolation is still a major design challenge existing in current mobile phones due to the magnificent difference between the level of the transmit power (say 0 dBm) and the sensitivity of a receiver (say -100dBm). A small leakage from the Tx to the Rx may burn the Rx circuit or least saturate it, thus degrading the Rx sensitivity. The Tx noise in the Rx spectrum also degrades the quality of the received signal and is often considered the dominant source of noise. The problem becomes more challenging when considering the following system scenarios:

- Frequency Division Duplex (FDD) systems like most cellular systems, including the UMTS/WCDMA, CDMA-2000 system and the IEEE 802.16 WiMax system. In such systems, the Tx and the Rx are simultaneously active over two neighboring subbands.
- Tx and Rx modules belonging to different wireless standards and collocated in the same handset, e.g. a GSM Tx collocated with a D-TV Rx.

To mitigate the Tx noise in the Rx spectrum, duplex filters should be sharp and able to provide a high level of isolation so as to perfectly isolate the neighboring subbands. Unfortunately, duplex filters are quite bulky whereas the proposed Surface Acoustic Wave (SAW) filters, though occupying smaller area, provide limited performance [5]. Moreover, duplex filters are generally narrowband thus, covering multiple wireless bands requires a bank of switched narrowband filters. This in turn increases size, cost as well as switching losses.

This paper exploits the balanced PA - antenna architecture for synthesizing a spatial filter that replaces the duplex filter or at least relaxes its requirement. The spatial filter is synthesized by equipping the Tx with at least one more antenna than the Rx. The Tx antennas are properly weighted such that the near-field is zero-forced in the direction(s) of the Rx antenna(s). The proposed approach combines the concept of leakage cancel-

[1] Antennas, Propagation and Radio Networking (APNet) Section, Department of Electronic Systems, Faculty of Engineering and Science, Aalborg University, DK-9220 Aalborg, Denmark (e-mails: {ona,ata,mp,gfp}@es.aau.dk).

[2] Intel Mobile Communication Denmark Aps, Aalborg East, Denmark (e-mail: mikael.knudsen@intel.com).

lation and antennas decoupling. Unlike conventional leakage cancellation that takes place right after the Rx antenna, the proposed approach selectively cancels the Tx power in the Rx direction (Tx spatial combining). Moreover, like conventional antennas decoupling techniques, the proposed approach diminishes the trans-impedance between the Tx and the Rx i.e. the Tx-Rx isolation is owed to the mutual coupling loss between the Tx and the Rx antenna(s). The spatial duplexing filter is shown to achieve a remarkable level of adaptive and agile isolation, without trading such isolation with other antenna design parameters like bandwidth or efficiency. Moreover, by co-designing the Tx antennas and the balanced Tx architecture existing in current and future mobile handsets, cost, size, complexity and insertion loss are all minimized.

Notation: In the following, boldface lower-case and upper-case characters denote vectors and matrices, respectively. The operators $(\cdot)^*$, $(\cdot)^{\mathrm{T}}$ designate complex conjugate and matrix transpose operators, respectively. The notation $\mathbf{0}_N$ indicates an $N \times N$ matrix of all zero entries whereas the notion $(\cdot)_{ij}$ returns the $\{i, j\}$ entry of the enclosed matrix. $\|\cdot\|$ denotes the Euclidean norm of the enclosed vector, $|\cdot|$ returns the absolute value whereas $\angle$ returns the angle. Finally, $\mathbb{C}$ denotes the set of complex numbers of the specified dimensions.

The rest of the paper is divided as follows: Section II describes conventional duplexing whereas Section III proposes the concept of spatial duplexing using baseband null-steering as well as analogue orthogonal weighting networks. Section IV discusses the degrees of freedom of such approach whereas Section V investigates the sensitivity of the phase and amplitude control on the isolation level. Section VI provides simulation results together with a fully operational measured prototype whereas Section VII concludes the paper.

II. Conventional Duplexing

The traditional approach of attenuating the Tx leakage signal and the Tx noise that lies in the Rx band, is to employ a duplex filter comprised of two filters combined before the antenna. The filter-branch in the Tx path stops the Tx noise component that lies in the Rx band and the filter-branch in the Rx path stops the Tx signal overloading the Rx (Rx desensitization).

A duplexer can be built in many ways using classical resonant circuits (e.g. ceramic or cavity resonators). Recently, duplexers are being built using multilayer technology with the use of slotline or microstrip line coupling structures to improve the level of integration. Other popular techniques include SAW filters and Film Bulk Acoustic Wave Resonator (FBAR) devices. The following summarizes the classical duplexer designs

- Lumped element filters. [9]–[15]
- Cavity duplexing filters [16]–[20]
- Ceramic duplexing filters [21]–[26]
- SAW duplexing filters [27]–[31]
- MicroElectroMechanical Systems (MEMS) devices [32]–[34]
- MEMS resonators [35]–[49]
- Stripline or microstrip line duplexing filters [50]–[55]

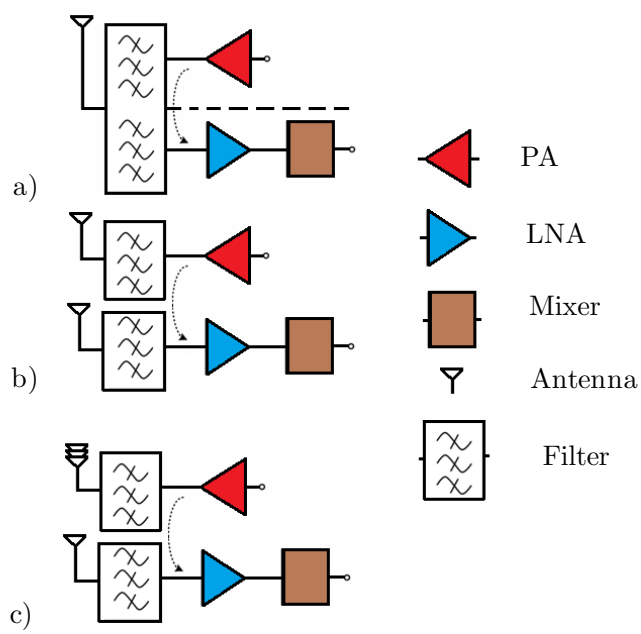

Fig. 1. Evolution of the spatial adaptive duplexing concept from conventional duplexing a), Tx-Rx separation mode b) and a spatial duplexing filter by equipping the Tx with multiple antennas.

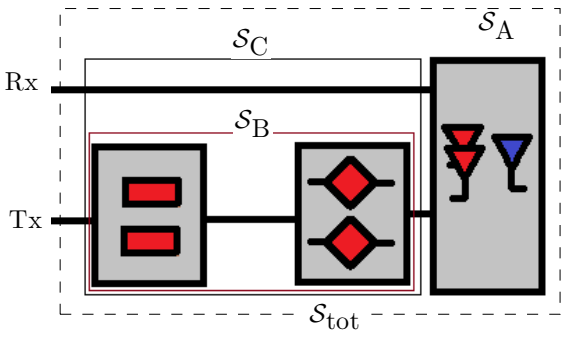

Fig. 2. Cascaded network of three port antenna setup $\mathcal{S}_{\mathrm{A}}$ with a power splitter and the phase shifter. The power splitter and a phase shifter form a balun $\mathcal{S}_{\mathrm{B}}$, which together with the Rx path are denoted as $\mathcal{S}_{\mathrm{C}}$. The total cascaded network is denoted by $\mathcal{S}_{\mathrm{tot}}$.

However, such filters are either bulky and thus are only appropriate for base stations rather than for handheld devices or suffer from a limited performance like the SAW filters. To make matters worse, all such filters are limited to one or few operational bands, thus a multiple-band state-of-the-art transceiver requires a bank of filters. Having a number of narrowband filters connected to the antenna through a switch is bulky and expensive while the switch adds further attenuation and induces intermodulation. Therefore, the current trend in designing such filters is to make the duplexer agile and adaptive using one of the following approaches:

- Tunable duplex filters [6]–[8].

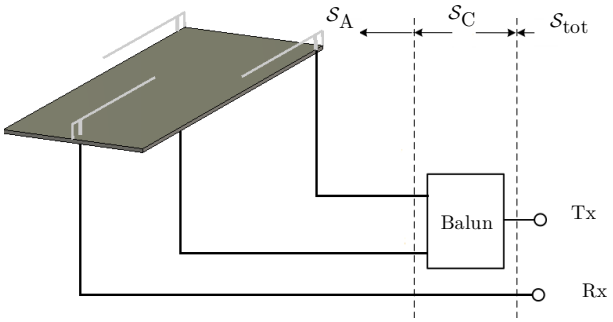

Fig. 3. Symmetric topology of three IFA antennas $\mathcal{S}_{\mathrm{A}}$, attached a balun which together with the Rx path form $\mathcal{S}_{\mathrm{C}}$.

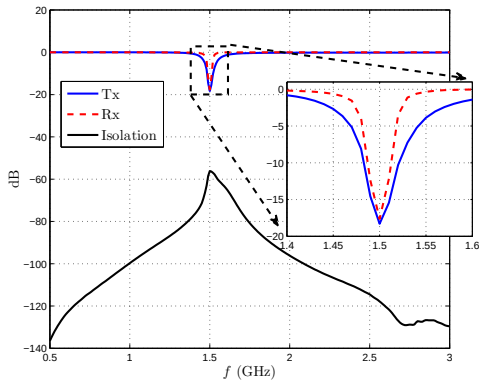

Fig. 4. Frequency response of the three IFA antennas setup where $\mathcal{S}_{\mathrm{TxTx}}$ is the Tx reflection coefficient, $\mathcal{S}_{\mathrm{RxRx}}$ is the Rx reflection coefficient and $\mathcal{S}_{\mathrm{TxRx}} = \mathcal{S}_{\mathrm{RxTx}}$ is the Tx-Rx coupling.

- Active filters: The idea here is to combine the Tx leakage with a scaled anti-phased version of the Tx signal i.e. equal amplitude and opposite phase, at the Rx frontend right after the Rx antenna. This can be done using single path feed-forward [56] [57] [58] or multiple paths [59]. The approach achieves high level of isolation but is not very promising as it requires accurate power detectors as well as accurate phase shifters and gain controllers. Moreover, this method degrades the Tx efficiency as some of the Tx energy is dissipated in the Rx circuit, unless initial Tx-Rx is provided. Besides complexity and inefficiency, small errors in the whole mechanism may lead to severe performance degradation.
- Antenna filters: A shift in the adaptive duplexing paradigm was proposed in [60] [61] where the conventional duplex filter requirements are relaxed by i) separating the Tx antenna from the Rx antenna and ii) equipping the Tx and the Rx with narrowband or high Quality (Q) factor antennas. In other words, the Tx-Rx isolation is partially due to the mutual coupling loss between the Tx and the Rx antennas. Moreover, high Q antennas can be tuned using simple variable capacitors mounted on the antenna structure itself or within the matching network. In fact, the Tx and the Rx antennas can be decoupled using many other techniques available in the literature like 1) antenna spacing and angular orientation variation [62]–[65], 2) decoupling networks [66]–[70], 3) parasitic and coupling elements [71]–[73], 4) defected ground-plane structures [74]–[78] and 5) neutralization lines [79]–[82]. However, most of such techniques, unlike the *narrowband* antenna decoupling concept, are difficult to tune or adjust in practice. The problem with all antennas decoupling methods (including the method of frequency

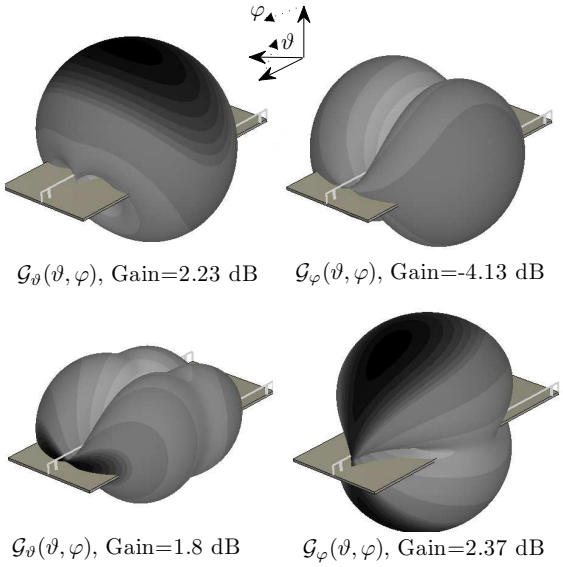

Fig. 5. Far-field beampattern (active gain) of the combined Tx and an ideal balun 1) and the Rx 2) where $\mathcal{G}_\vartheta$ and $\mathcal{G}_\varphi$ are the ϑ φ polarization components of the far-field.

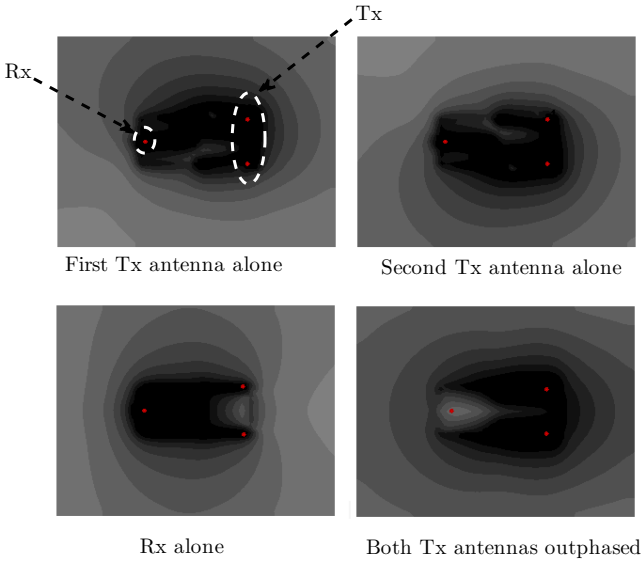

Fig. 6. The magnitude of the spatial power flow vector $|\vec{E} \times \vec{H}|$ when the exciting the first Tx antenna 1), the second Tx antenna 2), the Rx antenna 3) and the combined Tx antennas through an ideal balun.

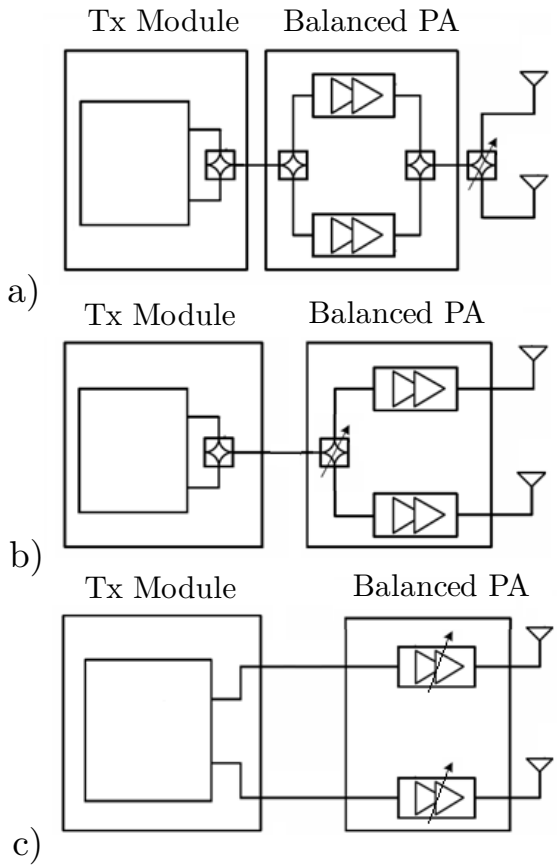

Fig. 7. Integration of the adaptive duplexing with the Tx RF frontend by adding a tunable balun/hybrid a), by directly connecting the PA balanced output to the antennas b) and by maintaining a balanced architecture all the way from the Tx module to the antennas via a balanced PA c).

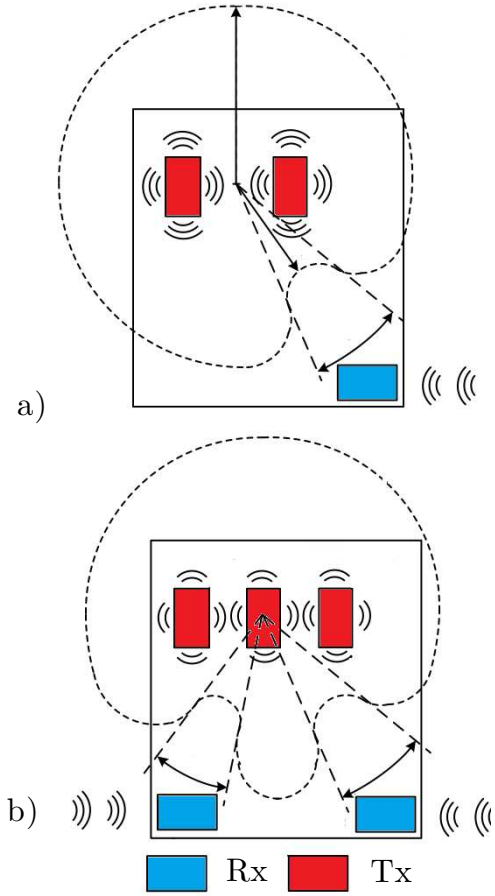

Fig. 8. Near-field null steering concept with two Tx - one Rx antennas setup a) and three Tx two Rx antennas setup b).

offsetting high Q antennas) is the limited level of isolation compared to leakage cancellation, especially in the low frequency bands like UMTS-FDD band XIII where the uplink operates at 777-787 MHz and the downlink at 746-756 MHz.

III. Spatial Duplexing

Spatial filtering using multiple antennas is a well established field in wireless communications [83], conventionally employed for canceling the interference via *far-field* null steering or zero forcing. For example, [84] [85] utilize the zero forcing concept for canceling the interference in the downlink channel. In this paper we borrow the concept of spatial filtering to design a self-duplexing antenna system that can safely operate without a traditional duplex filter or at least relax the design requirements of the filter. The evolution of the self-duplexing antenna design is shown in Fig. 1 where a) shows a conventional duplexing setup and b) allocates the Tx and the Rx separate antennas where partial isolation can be gained by offsetting the resonance of the Tx and Rx antennas. Finally, c) suggests equipping the Tx with multiple antennas for null steering the *near-field* in the Rx direction. Obviously such selective attenuation may not be enabled without multiple Tx antennas. Although it may seem that three antennas per transceiver is a costly design, this is still a low cost solution for obtaining adaptive and agile duplexing, dispensing with a bank of switched filters. Moreover, we show later that the two Tx antennas may naturally integrate with the Tx RF frontend thus effectively reducing the total cost and complexity rather than increasing them. The spatial duplexing can be performed with multiple RF sources or with a single RF source as follows:

A. Multiple RF Sources:

As previously mentioned, the idea we propose is to equip the mobile handset with a number of Tx antennas greater by at least one than the Rx antennas. Assume each Tx antenna has its separate RF chain and source. Moreover, the Tx and the Rx operate at the same frequency (worst case assumption), then the narrowband near-field channel transfer function between the Tx and Rx antennas at frequency f is given by $\mathbf{H}(f) \in \mathbb{C}^{\mathcal{K}_{\mathrm{R}} \times \mathcal{K}_{\mathrm{T}}}$ where $\mathcal{K}_{\mathrm{R}}$ is the number of the

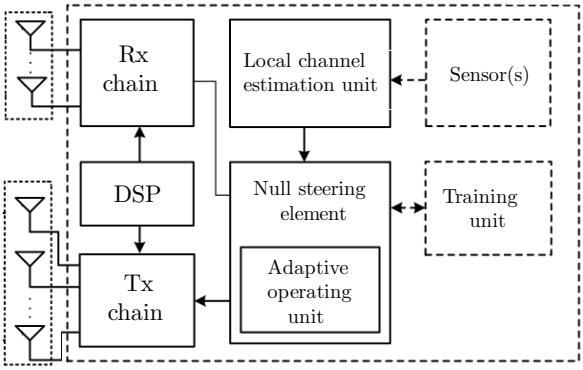

Fig. 9. A block diagram illustrating the interconnections among the digital sub-blocks required for local null steering.

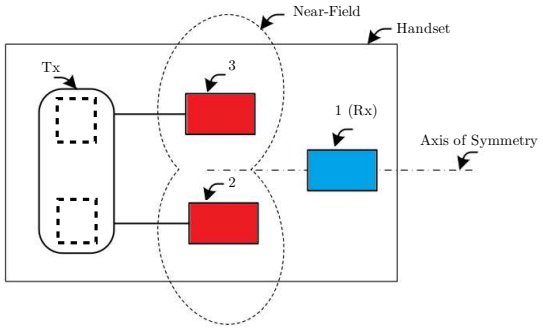

Fig. 10. Symmetric topology of three antennas (two Tx antennas and one Rx antenna) plus a balun. The Tx antennas are designated by ports 2 and 3 whereas the Rx antenna is designated by port 1. More Rx antennas can be placed on the axis of symmetry and stay isolated from the Tx as long as the symmetry is maintained.

Rx antennas and $\mathcal{K}_{\mathrm{T}}$ is the number of the Tx antennas. The frequency dependence is dropped hereinafter for simplicity. The spatial filter is formed by driving the Tx antennas with a precoding vector obtained from the kernel of $\mathbf{H}$, i.e. by properly weighting the Tx antennas, the Tx signal is projected in the noise subspace of $\mathbf{H}$. In case the nullity of the matrix $\mathbf{H}$ is greater than one, the extra degrees of freedom can be employed to multiplex more than one transmit signal.

A state-of-the-art approach for obtaining the kernel of a matrix is based on the singular value decomposition (SVD). The SVD algorithm can be programmed using standard libraries, such as LAPACK. The SVD operator of the matrix $\mathbf{H}$ computes unitary matrices $\mathbf{U}$ and $\mathbf{V}$ and a rectangular diagonal matrix $\mathbf{\Sigma}$ of the same size as $\mathbf{H}$ with nonnegative diagonal entries, such that

$$\mathbf{U}\mathbf{\Sigma}\mathbf{V}^{\mathrm{T}} = \mathbf{H}. \tag{1}$$

Denote the columns of $\mathbf{V}$ by $\mathbf{v}_1, \ldots, \mathbf{v}_{\mathcal{K}_{\mathrm{T}}}$ and the diagonal

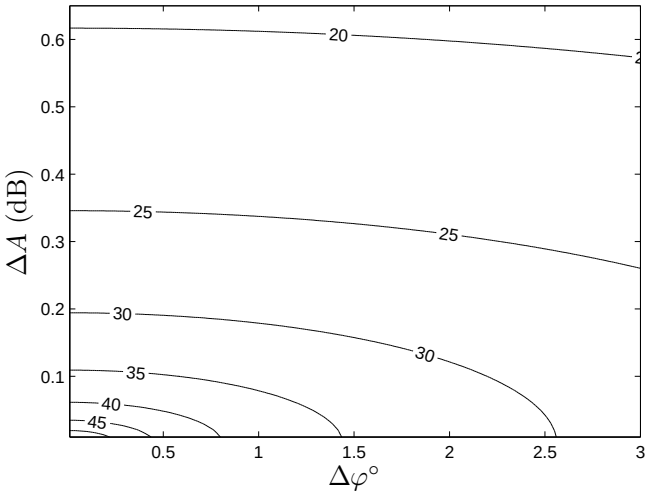

Fig. 11. Isolation dependence on amplitude and phase mismatch in the digital based isolation approach.

entries of $\mathbf{\Sigma}$ by $\sigma_1, \ldots, \sigma_{\min\{\mathcal{K}_{\mathrm{R}},\mathcal{K}_{\mathrm{T}}\}}$, where $\sigma_{\min\{\mathcal{K}_{\mathrm{R}},\mathcal{K}_{\mathrm{T}}\}+1} = \cdots = \sigma_{\max\{\mathcal{K}_{\mathrm{R}},\mathcal{K}_{\mathrm{T}}\}}$ are set to zero (σ_k are the singular values of $\mathbf{H}$). Then the column vectors $\mathbf{v}_k$ of $\mathbf{V}$ for which the corresponding $\sigma_k = 0$, form an orthonormal basis in the null subspace of $\mathbf{H}$. As an example, assume an Rx denoted by port 1 and two Tx antennas denoted by ports 2 and 3. The local channel from the Tx to the Rx is a row vector given by

$$\mathbf{H} = [\mathcal{S}_{21} \;\; \mathcal{S}_{31}], \tag{2}$$

from which the orthogonal precoding vector obtained via the SVD algorithm is given by the column vector

$$\left(\mathbf{v}_2 := \mathbf{v}^{\perp}\right) \propto [-\mathcal{S}_{31} \;\; \mathcal{S}_{21}]^{\mathrm{T}}. \tag{3}$$

The SVD of the matrix $\mathbf{H}$ is typically computed by a two-step procedure. The first step is the heaviest and it takes $\mathrm{O}(\mathcal{K}_{\mathrm{T}}\mathcal{K}_{\mathrm{R}}^2)$ floating-point operations (flops).

B. One RF Source:

In some hardware-constrained transceivers, driving the transmit antennas with equal but scaled versions of the same signal using multiple RF sources and corresponding RF chains could be seen as waste of real estate. To avoid the redundancy in such systems, the signal generated by *one* RF source is split into two (or more) feed branches where each branch is independently modulated in the RF stage via vector modulators or tunable phase shifters and gain controllers. This can be either done with a tunable *balun*, a tunable 3-dB rat-race coupler or a power divider together with a phase shifters. In this part we focus on the scenario of two transmit RF ports and one receive RF port, however scaling the analysis to a higher system order is straightforward. We assume the simplest scenario of two transmit RF ports (ports 2 and 3) that are symmetric with respect to the Rx port (port 1). The standard scattering matrix for such assumption is given by

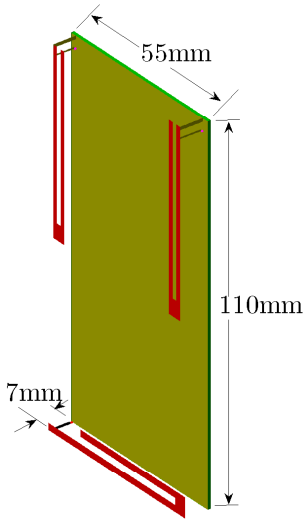

Fig. 12. The handset CAD model represented by a 55×110 mm PEC PCB (typical smart phone size) over which two Tx PIFA antennas and one Rx ILA antenna are installed.

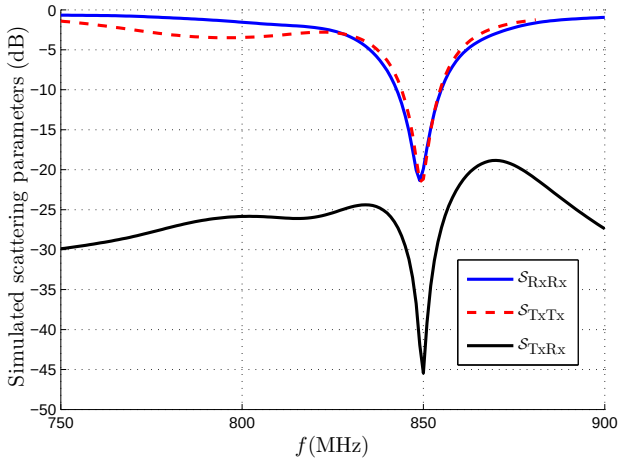

Fig. 13. Frequency response (simulation) of the handset model in Fig. 12 using our in-house FDTD code where $\mathcal{S}_{\mathrm{TxTx}}$ is the Tx reflection coefficient, $\mathcal{S}_{\mathrm{RxRx}}$ is the Rx reflection coefficient and $\mathcal{S}_{\mathrm{TxRx}} = \mathcal{S}_{\mathrm{RxTx}}$ is the Tx-Rx coupling.

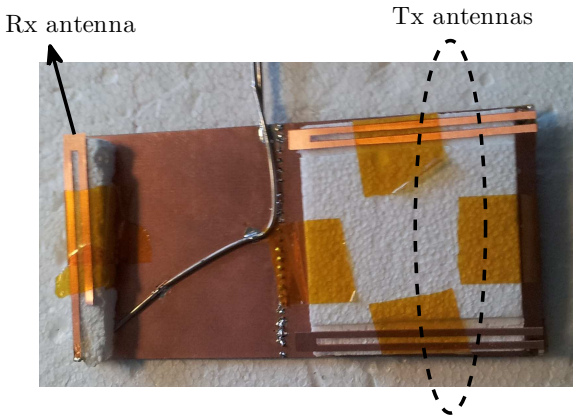

Fig. 14. The mock-up of the handset model in Fig. 12.

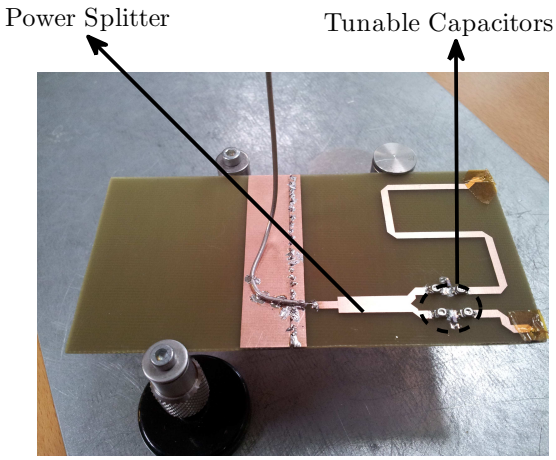

Fig. 15. The Tx-Rx isolation network printed on the backside of the handset mock-up.

$$\boldsymbol{\mathcal{S}}_{\mathrm{A}} = \begin{bmatrix} \mathcal{S}_{11} & \mathcal{S}_{12} & \mathcal{S}_{12} \\ \mathcal{S}_{12} & \mathcal{S}_{22} & \mathcal{S}_{23} \\ \mathcal{S}_{12} & \mathcal{S}_{23} & \mathcal{S}_{22} \end{bmatrix}, \tag{4}$$

where $\{\boldsymbol{\mathcal{S}}_{\mathrm{A}}\}_{22} = \{\boldsymbol{\mathcal{S}}_{\mathrm{A}}\}_{33}$ and $\{\boldsymbol{\mathcal{S}}_{\mathrm{A}}\}_{12} = \{\boldsymbol{\mathcal{S}}_{\mathrm{A}}\}_{13}$ by the assumption of having symmetric topology and identical Tx antennas. It is intuitive that splitting the transmit signal into two equal halves and out-phasing one half by 180°, the Tx signal will lie in the kernel of $\mathbf{H}$. To illustrate this, Fig. 2 shows how a balun $\boldsymbol{\mathcal{S}}_{\mathrm{B}}$ (comprised by cascading a power splitter and a phase shifter) is inserted in the transmit path (denoted by Tx). The balun operation together with the Rx feed is expressed as

$$\boldsymbol{\mathcal{S}} = \begin{bmatrix} \mathbf{0}_2 & \boldsymbol{\mathcal{S}}_{\mathrm{C}}^{\mathrm{T}} \\ \boldsymbol{\mathcal{S}}_{\mathrm{C}} & \mathbf{0}_3 \end{bmatrix}, \tag{5}$$

where

$$\boldsymbol{\mathcal{S}}_{\mathrm{C}} = \begin{bmatrix} +1 & 0 \\ 0 & \frac{+1}{\sqrt{2}} \\ 0 & \frac{-1}{\sqrt{2}} \end{bmatrix}, \tag{6}$$

assuming ideal 3dB splitter with isolated outputs and matched inputs/outputs. By cascading $\boldsymbol{\mathcal{S}}_{\mathrm{C}}$ with $\boldsymbol{\mathcal{S}}_{\mathrm{A}}$ the total scattering matrix becomes

$$\begin{aligned} \boldsymbol{\mathcal{S}}_{\mathrm{tot}} &= \boldsymbol{\mathcal{S}}_{\mathrm{C}}^{\mathrm{T}} \boldsymbol{\mathcal{S}}_{\mathrm{A}} \boldsymbol{\mathcal{S}}_{\mathrm{C}} \\ &= \begin{bmatrix} \mathcal{S}_{11} & 0 \\ 0 & \mathcal{S}_{22} - \mathcal{S}_{23} \end{bmatrix} \\ &:= \begin{bmatrix} \mathcal{S}_{\mathrm{RxRx}} & \mathcal{S}_{\mathrm{RxTx}} \\ \mathcal{S}_{\mathrm{TxRx}} & \mathcal{S}_{\mathrm{TxTx}} \end{bmatrix}. \end{aligned} \tag{7}$$

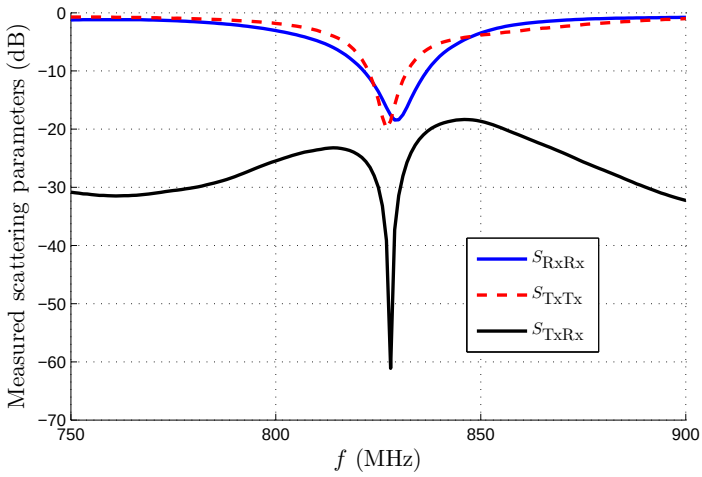

Fig. 16. Frequency response (measurements) of the handset mock-up in Fig. 14 exported from the vector network analyzer where $\mathcal{S}_{\mathrm{TxTx}}$ is the Tx reflection coefficient, $\mathcal{S}_{\mathrm{RxRx}}$ is the Rx reflection coefficient and $\mathcal{S}_{\mathrm{TxRx}} = \mathcal{S}_{\mathrm{RxTx}}$ is the Tx-Rx coupling.

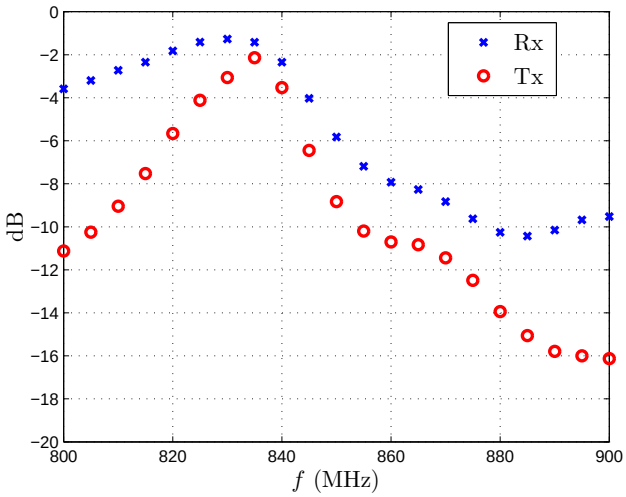

Fig. 18. Total efficiency of both the Tx and the Rx including all the losses in the antennas and the decoupling network. The data is exported from the `Satimo Starlab®`.

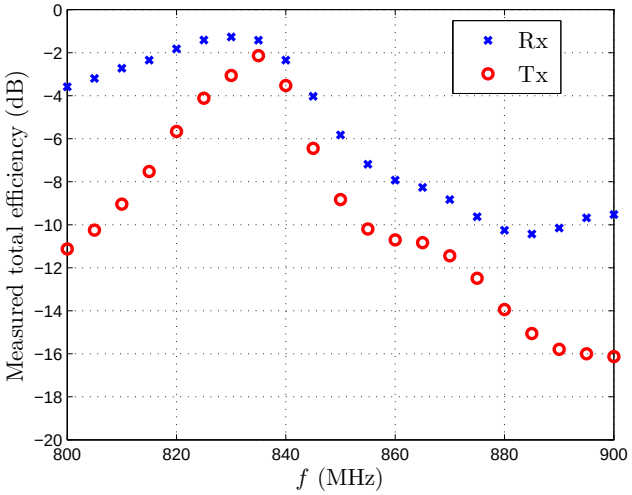

Fig. 17. The mock-up inside the `Satimo Starlab®` for total efficiency measurements.

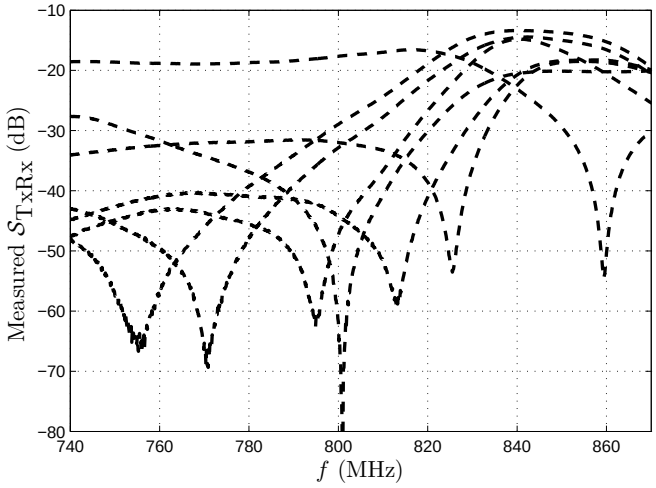

Fig. 19. Demonstrating agile duplexing by tuning $\mathcal{S}_{\mathrm{TxRx}}$ over a band of 100 MHz band.

Illustrative Example: To have a deeper insight on the near and the far fields when driving a symmetric antenna topology with a balun, we consider a three Inverted F Antennas (IFAs) over a 40×100mm Printed Circuit Board (PCB) representing the typical dimensions of a bar-type mobile phone, as shown in Fig. 3. The top pair antennas are the Tx and the lower one is the Rx. The IFA antennas have a height of 4mm and a length of 40mm. The relative distance between the feed and the short is optimized such that the Tx (after combining the ports using an ideal balun) as well as the Rx, both resonate at 1.5 GHz. Fig. 4 shows the frequency response of the setup example where an isolation of 55 dB was obtained. Fig. 5 shows the active gains of the Tx and the Rx. It is found that the Tx ϑ polarization component is orthogonal to the Rx ϑ polarization component and the same applies to the φ polarization components. Such observations agree with the fundamental result in [86] which states that the port patterns of any lossless decoupled antenna system are orthogonal. Last but not least, Fig. 6 plots the magnitude of the spatial power flow given by $|\vec{E} \times \vec{H}|$ where $\vec{E}$ and $\vec{H}$ are the electric and magnetic fields, respectively. The power flow is shown in a 2D plane (the lighter the color the lower the power level) for the first Tx antenna, the second Tx antenna, the Rx antenna and the combined Tx. The last figure clearly illustrates the near-field null steering concept where a null (bright spot) appears over the location of the Rx antenna though each Tx antenna is coupled individually to the Rx antenna.

Antenna frontend co-design: Often the PA output in LTE, UMTS or GSM is obtained by combining two PA modules with a hybrid on the input and the output of the PA module.

On the Tx side, all the signals are balanced and there is a hybrid at the output of the Tx module to convert it into single ended. With this implementation, a tunable balun/hybrid is needed at the PA output to implement the near-field zero forcing concept as shown in Fig. 7a. Alternatively, as Fig. 7a presents the standard perception of the implementation with no modifications to the frontend, Fig. 7b shows a possible intermediate setup where the balanced antenna is directly attached to the balanced PA output as in [3].

On the other hand, the zero forcing concept can be implemented digitally by removing all the hybrids throughout the Tx chain, see Fig. 7c. With this lineup, no hybrid couplers will be required on the input or the output of the PA module. The hybrid at the Tx output is removed and the zero forcing is done digitally without the need for a tunable balun/hybrid, all-in-all resulting in a significant reduction in the total insertion loss. In an all-digital Tx modulator, a phase shift of one branch relative to the other can be done relatively simple by a register shift operation. A variable phase shift can be applied digitally to one of the branches in the PA module, which can be used to phase shift the signal at one antenna output relative to the other. By adjusting the relative phase shift of the transmitted signal from one antenna relative to the other it is possible to adjust the relative phase of the two versions of the Tx signal. Moreover, it is possible to adjust the power level of each transmitted signal by using independent power control of the two Tx signals. By adjusting both phase and amplitude it is possible to implement the zero forcing concept digitally and using one RF source.

IV. Degrees of Freedom

A. Time-varying channel

In case the entries of the matrix $\mathbf{H}$ are time-varying by the near-field coupling with nearby objects e.g. the proximity effect of the user head and hand, the nullity of $\mathbf{H}$ is given by $\mathcal{K}_{\mathrm{T}} - \mathcal{K}_{\mathrm{R}}$. To illustrate this, Fig. 8a shows a setup of two Tx antennas and one Rx antenna, thus the system has a nullity of one, i.e. the Tx can transmit one signal subject to staying orthogonal to the Rx direction. Fig. 8b shows a system with three Tx antennas and two Rx antennas, again the nullity is one thus one Tx signal can be transmitted while two signals can be received without suffering from any harmful Tx leakage. In Fig. 8b, if the Rx has one antenna, then the nullity of $\mathbf{H}$ is two and two independent Tx signals can thus be multiplexed while staying orthogonal to the Rx antenna.

On the other hand, learning the local time-varying channel requires lowering the Tx power during the training phase to a level that does not harm the Rx sensitivity. Another training strategy is to use a pseudo-random pilot signal where the signal power is lowered by spreading it over a wide spectrum band. Fig. 9 shows the relation among the system subblocks required for learning the channels and for weighting the Tx antennas. Alternatively, the zero-forcing approach can be performed blindly without learning the channel; by iterating Rx power and the Tx weights until converging into an acceptable level of isolation.

The rate over which the weights should be updated depends on the rate over which isolation (i.e. the Tx-Rx leakage in dBm) is degraded. This rate is expected to be much slower than the rate over which the far-field channel gains vary in a scattering environment. The isolation could be either enhanced or degraded by the proximity effect of the user head and hand depending on the exact setup and the type of the antennas. For example, the impedance mismatch when using narrowband antennas is quite insignificant compared to the absorption losses by the user hand. Such losses enhance the Tx-Rx isolation. Moreover, the fact that the closed loop mechanism for sensing the leakage and updating the weights is local in the same handset, the time-delay required for maintain the isolation becomes negligible [61]. Last but not least, the fact that the closed loop mechanism for sensing the leakage and updating the weights is local in the same handset, the time-delay required for maintain the isolation becomes negligible.

B. Time-invariant channel

In case the elements of the matrix $\mathbf{H}$ are constant (static channel), multiple Rx antennas can be isolated from the Tx antennas by properly exploiting the antenna location. To illustrate this, Fig. 10 illustrates two Tx antennas that are symmetric with respect to the Rx antenna, thus $\mathbf{H} = [\mathcal{S}_{21}\ \mathcal{S}_{21}] = \mathcal{S}_{21}\,[1\ 1]$. It is obvious that by driving the two Tx antennas with equal but out of phase excitations (180° difference in phase), full Tx-Rx isolation is obtained. Moreover, an infinite number of Rx antennas can be placed on the axis of symmetry shown in the figure and enjoy a high level of isolation. This is because any Rx antenna placed on this axis will have a local channel vector $\mathbf{H}'$ proportional to $\mathbf{H}$ (equal to *all ones* up to a scalar), and thus any weighting vector orthogonal to $\mathbf{H}$ will be orthogonal to $\mathbf{H}'$.

V. Sensitivity Analysis

We theoretically investigate the error in the weighting vector applied to the Tx antennas on the Tx-Rx isolation. To do so, we consider the system example in Fig. 10 where the two Tx antennas are weighted with the vector $\mathbf{v} = [v_1\ v_2]$ such that $\|\mathbf{v}\|^2 = 1$. The relationship between the voltage signal squared at the Rx to the transmit Tx voltage signal squared when driving the Tx antennas with an arbitrary excitation vector $\mathbf{v} = [v_1\ v_2]$ becomes after some manipulations as follows

$$|V_{\mathrm{Rx}}|^2 = |V_{\mathrm{Tx}}|^2 \left(1 - \frac{2\,(\Delta A)}{1 + (\Delta A)^2}\cos(\Delta\phi)\right) \qquad (8)$$

where $\Delta\ A$ and $\Delta\phi$ are the amplitude imbalance and phase deviation from 180°, respectively. Fig. 11 shows the isolation level in dB, i.e. $10\log_{10}\left(\frac{|V_{\mathrm{Rx}}|}{|V_{\mathrm{Tx}}|}\right)$ versus ΔA and $\Delta\phi$. The minimum amplitude mismatch was set to 0.01 dB and the minimum phase mismatch (from 180°) was set to 0.01 degrees. The figure shows that around $35 - 40$ dB of isolation is obtained with a maximum amplitude mismatch of 0.1 dB jointly with a maximum phase mismatch of of 1.5°. Although the matching of the amplitude and phase seems to be strict, such matching is obtained digitally within a remarkable resolution whereas obtaining such accuracy in practice is done by tuning the two feeds rather than one. Later we show that with two tunable

capacitors per feed, the null is *continuously* steered over a frequency band of 100 MHz though no attempt was attained to optimize the isolation level over such band.

VI. Antenna Design and Measurements

The numerical simulations were conducted using our in-house Finite Difference Time Domain (FDTD) code, choosing a space step size of 1mm and an energy based termination criterion. The FDTD code is parallel and it uses the supercomputer facilities at Aalborg University (Fyrkat) [87], allowing demanding simulations to be run in a limited time. The handset ground-plane has been modeled as a Perfect Electric Conductor (PEC) plate representing the typical dimensions of a smart phone (55mm $\times$ 110mm). A practical implementation has been considered and intended for the extreme scenario of i) zero duplex separation together with ii) operation in the low frequency band. The computer aided design (CAD) model is shown in Fig. 12 where three simple structures have been used as radiators, two of them are Planar Inverted F Antennas (PIFAs) whereas the third is an Inverted L Antenna (ILA). Slots in the antenna structures are introduced to reduce the antenna dimensions at the expense of bandwidth. The height of the antennas is 7 mm occupying an area of 6×55 mm^2. The model is reused to construct a feeding network on the backside which is required for the Tx-Rx isolation. The network was co-simulated using `Agilent ADS`® and used to feed PIFAs on the other side of the PCB. The networks is comprised of a power splitter, two T networks and transmission lines. The lengths of the transmission lines were optimized so that a null appears in the Rx (the ILA) direction at the resonance frequency. This phase difference can be smoothly tuned using some tunable capacitors within the T network. The T network has two tunable capacitors with a shunt inductor connected to the ground. The Q of the components used in the manufacturing are 90 and 80 for the inductors and the capacitors, respectively. The network has a small tuning range of 20° over which the insertion loss is maintained low (the insertion loss of the feeding network ranges from $1-2.5$ dB depending on the capacitors' settings.) while the difference in the length of the transmission lines provides the desired phase shift value. The slight tuning in the T network is meant to have some agility around the major target band. The frequency response of the simulated model is shown in Fig. 13 where a deep null is obtained at the desired band by slightly tuning the capacitors.

With these specification, a prototype has been manufactured as shown in Fig. 14. The antenna elements are stabilized using polystyrene and Teflon tapes whereas the PCB is a two sided FR4. The isolation network is synthesized over the backside of the PCB as shown in in Fig. 15. Thin coaxial cables have been used for feeding and measuring the mock-up. The cables are led away from the PCB in a direction orthogonal to the main current oscillation path thus limiting the cable effects. Fig. 16 shows the frequency response of the measured prototype where a good agreement between simulation and measurements is obtained, except for a 20 MHz difference due to the numerical dispersion in the FDTD domain besides some possible manufacturing imperfections. The level of isolation is impressive considering an initial coupling of -4 dB between the PIFAs and around -5 dB between the PIFAs and the ILA.

The total efficiency of the system has been measured using the `Satimo Starlab`® shown in Fig. 17. The total efficiency curve is shown in Fig. 18, includes the losses in the antennas as well as the losses in the feeding network and cables. The curve is generally calculated by integrating the 3D far-field (power) radiation patterns. From the total efficiency curve, the bandwidth of the Tx antenna configuration is found smaller than the Rx bandwidth mainly due to limiting the current distribution over some parts of the PCB (the area where the Rx resides). Finally Fig. 19 shows how the null is tuned over a band of 100 MHz (though no attempts were made to optimize the performance of the isolation network over such band) paving the way for agile duplexing.

VII. Conclusion and Future Work

The paper proposed the concept of spatial duplexing for isolating the Tx from the Rx in a local handset, utilizing the balanced Tx architecture in mobile phones. The immensely attained Tx-Rx isolation is not traded for other antenna parameters like bandwidth and efficiency while the co-design of the proposed concept with the RF frontend gets rid of baluns or hybrid couplers that incur unnecessary losses and occupy a large space.

In the future we aim at performing a complete modeling of the impedance parameters (local coupling channel coefficients), and evaluate their rate of change within a normal user coupling environment utilizing the APNet unique optical units [88]. We will also investigate the proximity effect by the user on the spatial filter performance and study the role of the antenna type on such isolation. Finally we are aiming at validating the spatial duplexing concept through a real-time demonstration.

VIII. Acknowledgment

The work is supported by the Smart Antenna FrontEnd (SAFE) project within the Danish National Advanced Technology Foundation - High Technology Platform.

References

[1] V. Savov, "IPhone 4 antenna problems were predicted on June 10 by Danish professor," Online Available (Yellow Paper), Jun., 2010.

[2] E. Tsakalaki, O. N. Alrabadi, C. B. .Papadias and R. Prasad, "Spatial Spectrum Sensing for Wireless Handheld Terminals: Design Challenges and Novel Solutions Based on Tunable Parasitic Antennas," *IEEE Wireless Communications Magazine*, vol.17, no. 4, pp. 33-40, August 2010.

[3] W. R. Deal, V. Radisic, Q. Yongxi, T. Itoh, "Integrated-antenna pushpull power amplifiers," *IEEE Trans. on Microwave Theory and Techniques*, pp. 1418 - 1425, vol. 47, no. 8, Aug 1999.

[4] S. Kingsley, "Advances in Handset Antenna Design," Online Available: *www.rfdesign.com*, pp. 16-22, May 2005.

[5] J. Machui, J. Bauregger, G. Riha and I. Schropp, "SAW devices in cellular and cordless phones," *IEEE Ultrasonics Symposium*, pp. 121-130, vol. 1, 1995.

[6] A. Abbaspour-Tamijani, L. Dussopt, and G. M. Rebeiz, "A high performance MEMS miniature tunable bandpass filter," *IEEE MTT-S Int. Microwave Symp. Dig.*, Jun. 813, 2003, pp. 17851788.

[7] B. Lakshminarayanan and T. Weller, "Tunable bandpass filter using distributed MEMS transmission lines," *IEEE MTT-S Int. Microwave Symp.* Dig., vol. 3, Jun. 813, 2003, pp. 17891792.

[8] K. Saitou and K. Kegeyama, "Tunable duplexer having multilayer structure using LTCC," *IEEE MTT-S Int. Microwave Symp. Dig.*, vol. 3, Jun. 813, 2003, pp. 17631766.

[9] J.-S. Hong and M. J. Lancaster, *Microstrip Filters for RF/Microwave Applications*, John Wiley & Sons, Inc., 2001.

[10] Temex, RF Filters, Duplexers & Subassemblies.

[11] R. Levy, R. V. Snyder, and G. Matthaei, "Design of Microwave Filters," *IEEE Transactions on Microwave Theory and Techniques*, vol. 50, no. 3, pp. 783-793, March 2002.

[12] A. Coon, "SAW Filters and Competitive Technologies: A Comparative Review," *IEEE Proceedings of Ultrasonics Symposium*, vol.1, 8-11, pp. 155160, Dec. 1991.

[13] A. N. Mohieldin, E. Sanchez-Sinencio, and J. Silva-Martinez, "A 2.7-V 1.8-GHz Fourth-Order Tunable LC Bandpass Filter Based on Emulation of Magnetically Coupled Resonators," *IEEE Journal of Solid-State Circuits*, vol. 38, no. 7, pp. 1172-1181, July 2003.

[14] F Dulger, E. Sanchez-Sinencio, and J. Silva-Martinez, "A 1.3-V 5-mW Fully Integrated Tunable Bandpass Filter at 2.1 GHz in 0.35-/spl mu/m CMOS," *IEEE Journal of Solid-State Circuits*, vol. 38, no. 6, pp. 918-928, June 2003.

[15] A. Simine, *et al*., "Design of Quasi-Lumped-Element LTCC Filters and Duplexers for Wireless Communications," *33rd European Microwave Conference*, vol. 3, pp. 911914, Oct. 2003.

[16] K. Shoemaker, Cavities and Duplexer, www.dalek.org/srg/cavity.html

[17] RFI, Cavity Filters, www.rfi.com.au

[18] Chapter 17 - Repeater Antenna Systems

[19] F. L. William, EMR Corporation, Understanding, Maintaining & Re-Tuning Antenna Duplexers, www.emrcorp.com

[20] Radio Frequency Systems (RFS), *Duplexers-GSM 1800*, http://www.rfsworld.com/

[21] I. C. Hunter, L. Billonet, B. Jarry, and P. Guillon, "Microwave Filters-Applications and Technology," *IEEE Transactions on Microwave Theory and Techniques*, vol. 50, no. 3, pp. 794805, March 2002.

[22] J. Yohannan, A. V. P. Kumar, V. Hamsakkutty, V. Thomas, and K. T. Mathew, "Synthesis of Dielectric Resonator for Microwave Filter Designing," *Progress In Electromagnetics Research Symposium*, Hangzhou, China, Aug. 2005.

[23] C. Kudsia, R. Cameron, and W.C. Tang, "Innovations in Microwave Filters and Multiplexing Networks for Communications Satellite Systems," *IEEE Transactions on Microwave Theory and Techniques*, vol. 40, no. 6, pp. 11331149, June 1992.

[24] High Frequency Electronics, "Basic Data on High-Q Ceramic Coaxial Resonators," *High Frequency Electronics*, *Summit Technical Media*, LLC, p. 50, November 2002.

[25] TOKO, *Toko's TDP is a Chip Ceramic Dielectric*, http://www.toko.com/.

[26] Murata Manufacturing Co., Ltd., *Murata Products for Mobile Communications*, http://www.murata.com/

[27] J. Phillips, "Piezoelectric Technology Primer", Microwave Journal, Aug. 2001.

[28] T. Senbo, "Advanced SAW Filters Facilitate Design of Smaller Mobile Terminals," Technology Focus, Dempa Publications, pp. 45-53, Dec. 2003.

[29] D. Hao, T. X. Wu, K. S. Cheema, B. P. Abbott, C. A. Finch, and H. Foo, "Design of Miniaturized RF SAW Duplexer Package," *IEEE Transactions on Ultrasonics, Ferroelectrics and Frequency Control*, vol. 51, no. 7, pp. 849858, July 2004.

[30] G. Kovacs, W. Ruile, M. Jakob, U. Rosler, E. Maier, U. Knauer, and H. Zoul, "A SAW Duplexer with Superior Temperature Characteristics for US-PCS," *IEEE Ultrasonics Symposium*, vol. 2, pp. 974977, Aug. 2004.

[31] M. Kadota, T. Nakao, N. Taniguchi, E. Takata, M. Mimura, K. Nishiyama, T. Hada, and T. Komura, "SAW duplexer for PCS in US with Excellent Temperature Stability," *IEEE Symposium on Ultrasonics*, vol. 2, pp. 2105-2109, Oct. 2003.

[32] E. R. Brown, "RF-MEMS Switches for Reconfigurable Integrated Circuits," *IEEE Transactions on Microwave Theory and Techniques*, vol. 46, no. 11, Part 2, pp. 18681880, Nov. 1998.

[33] J. Bryzek, K. Petersen and W. McCulley, "Micromachines on the March," *IEEE Spectrum Magazine*, vol. 31, no. 5, pp. 2031, May 1994.

[34] Mumor, Design Methodology and Technologies for Multi-Mode Radio Front-Ends [On-line].

[35] S. Mishin, Y. Oshmyansky, J. D. Larson, and R. Ruby, *Sputtering Processes for Bulk Acoustic Wave Filters*.

[36] W. Mueller, "A Brief Overview of FBAR Technology", *White Paper*, *Agilent Technologies*.

[37] W. W. Lau, Y. Song, and E. S. Kim, "Lateral-Field-Excitation Acoustic Resonators For Monolithic Oscillators and Filters," *Proceedings of the 50th IEEE International Frequency Control Symposium*, pp. 558562, June 1996.

[38] K. M. Lakin, G. R. Kline, and K. T. McCarron, "High Q Microwave Acoustic Resonators and Filters," *IEEE Transactions on Microwave Theory and Techniques*, vol. 41, no. 12, pp. 21392146, Dec. 1993.

[39] K. M. Lakin, "Thin Film Resonator Technology," *Proceedings of the 2003 IEEE International Frequency Control Symposium and PDA Exhibition Jointly with the 17th European Frequency and Time Forum*, pp. 765778, May 2003.

[40] K. M. Lakin, G. R. Kline and K. T. McCarron, "Development of Miniature Filters for Wireless Applications," *IEEE Transactions on Microwave Theory and Techniques*, vol. 43, no. 12, Part 2, pp. 29332939, Dec. 1995.

[41] R. J. Richards and H. J. De Los Santos, "MEMS for RF/Microwave Wireless Applications: The Next Wave," *Microwave Journal*, March 2001.

[42] C. H. Tai, T. K. Shing, Y. D. Lee, and C. C. Tien, "A Novel Thin Film Bulk Acoustic Resonator (FBAR) Duplexer for Wireless Applications," *Tamkang Journal of Science and Engineering*, vol. 7, no. 2, pp. 67-71, 2004.

[43] R. Ruby, et al., "High Rejection Rx Filters for GSM Handsets with Wafer Level Packaging," *IEEE Proceedings of Ultrasonics Symposium*, vol. 1, pp. 925929, Oct. 2002.

[44] P. D. Bradley, et al., "Duplexer Incorporating Thin-Film Bulk Acoustic Resonators (FBARs)," U. S. Patent 6 262 637, July 17 2001.

[45] P. Bradley, R. Ruby, J. D. Larson, Y. Oshmyansky, and D. Figueredo, "A Film Bulk Acoustic Resonator (FBAR) Duplexer for USPCS Handset Applications," *IEEE MTT-S Internationa Microwave Symposium Digest*, vol. 1, pp. 367-370, 2001.

[46] R. Ruby, P. Bradley, J. D. Larson, and Y. Oshmyansky, "PCS 1900 MHz Duplexer Using Thin Film Bulk Acoustic Resonators (FBARs)," *Electronics Letters*, vol. 35, no. 10, pp. 794795, May 1999.

[47] S. Kim, J. Lee, H. Choi, and Y. Lee, "The Fabrication of Thin-Film Bulk Acoustic Wave Resonators Employing a ZnO/Si Composite Diaphragm Structure Using Porous Silicon Layer Etching, *IEEE Electron Device Letters*, vol. 20, no. 3, pp. 113115, March 1999.

[48] C. T. C. Nguyen, "Frequency-Selective MEMS for Miniaturized Low-Power Communication Devices," *IEEE Transactions on Microwave Theory and Techniques*, vol. 47, no. 8, pp. 14861503, Aug. 1999.

[49] L. E. Larson, "Microwave MEMS Technology for Next-Generation Wireless Communications," *IEEE MTT-S International Microwave Symposium Digest*, vol. 3, pp. 1073-1076, June 1999.

[50] G. Gonzalez, *Microwave Transistor Amplifiers Analysis and Design*, Second Edition, Prentice Hall, Upper Saddle River, New Jersey, 1997.

[51] H. Jia-Sheng and M. J. Lancaster, "Theory and Experiment of Novel Microstrip Slow-wave Open-Loop Resonator Filters," *IEEE Transactions on Microwave Theory and Techniques*, vol. 45, no. 12 Part 2, pp. 2358-2365, Dec. 1997.

[52] Y. Toutain, J. P. Coupez, and C. Person, "Microstrip Miniaturized Loop-Filters with High Out-Of-Band Rejection for Future 3G Mobile Terminals," *IEEE MTT-S International Microwave Symposium Digest*, vol. 3, pp. 15891592, May 2001.

[53] H. K. Yang, H. M. Cho, and J. C. Park, "The Effects of Stripline Geometries for Phase Shifting on SAW Antenna Duplexer, IEEE Proceedings of Ultrasonics Symposium, vol.1, pp. 115118, Oct. 1998.

[54] O. Ikata, et al., "Development of Small Antenna Duplexer using SAW Filters for Handheld Phones," *IEEE Proceedings of Ultrasonics Symposium*, vol. 1, pp. 111114, 31 Oct.-3 Nov. 1993.

[55] N. Hirasawa, H. Fukushima, O. Kawachi, T. Nishihara, O. Ikata, and Y. Satoh, "A Study of Miniaturization Technique of SAW Antenna Duplexer for Mobile Application," *IEEE Ultrasonics Symposium*, vol. 1, pp. 413416, Oct. 2000.

[56] T. OSullivan, R. York, B. Noren, and P. Asbeck, "Adaptive duplexer implemented using feedforward technique with BST phase shifter," *IEEE MTT-S Int. Microwave Symp.*, 2004.

[57] S. Kannangara and M. Faulkner, "Adaptive duplexer for multiband transceiver," *IEEE Radio and Wireless Conf.*, Aug. 1013, 2003, pp. 381384.

[58] S. Chen, M. A. Beach, and J. P. McGeehan, "Division-free duplex for wireless application," *Electron. Lett.*, vol. 34, no. 2, pp. 147148, Jan. 1998.

[59] T. OSullivan, R. York, B. Noren, and P. Asbeck, "Adaptive duplexer implemented using single-path and multipath feedforward techniques with BST phase shifters," *IEEE Trans. on Mic. Theory and Tech.*, vol. 53, no. 1, Jan. 2005.

[60] M. Pelosi, G. F. Pedersen and K. M. Bergholz, "A novel paradigm for high isolation in multiple antenna systems with user's influence," *4th European Conference on Antennas and Propagation (EuCAP)*, pp. 1-5, Jul. 2010.

[61] M. Pelosi, M. B. Knudsen, G. F. Pedersen, "Multiple antenna systems with inherently decoupled radiators," *IEEE Trans. on ant. and propag.*, pp. 503-515, vol. 60, no. Feb. 2012.

[62] P. Vainikainen, J. Holopainen, C. Icheln, O. Kiveks, M. Kyr, M. Mustonen, S. Ranvier, R. Valkonen, and J. Villanen, "More than 20 antenna elements in future mobile phones, threat or opportunity," Proceedings of the *3rd European Conference on Antennas and Propagation (EuCAP'2009)*, pp. 2940-2943, Mar. 2009.

[63] K. L. Wong, J. H. Chou, S. W. Su, and C. M. Su, "Isolation between GSM/DCS and WLAN antennas in a PDA phone," *Microwave Opt. Technol. Lett.*, vol. 45, p. 347, 2005.

[64] H. Carrasco, H. D. Hristov, R. Feick, and D. Cofr, "Mutual coupling between planar inverted-F antennas," *Microwave Opt. Technol. Lett.*, vol. 42, no. 3, pp. 224-227, Aug. 2004.

[65] A. Diallo , C. Luxey , P. L. Thuc , R. Staraj and G. Kossiavas, "Enhanced two-antenna structures for universal mobile telecommunications system diversity terminals", *IET Microw., Antennas Propag.*, vol. 2, no. 1, pp. 93-101, 2008.

[66] C. Volmer, J. Weber, R. Stephan, K. Blau, and M. A. Hein, "An eigenanalysis of compact antenna arrays and its application to port decoupling," *IEEE Transactions on Antennas and Propagation*, vol. 56, no. 2, pp. 360-370, Feb. 2008.

[67] B. K. Lau, J. B. Andersen, G. Kristensson, and A. F. Molisch, "Impact of matching network on bandwidth of compact antenna arrays," *IEEE Transactions on Antennas and Propagation*, vol. 54, no. 11, pp. 3225-3238, Nov. 2006.

[68] J. B. Andersen and H. Rasmussen, "Decoupling and descattering networks for antennas," *IEEE Transactions on Antennas and Propagation*, vol. 24, no. 6, pp. 841-846, Nov. 1976.

[69] S. C. Chen, Y. S. Wang and S. J. Chung, "A decoupling technique for increasing the port isolation between two strongly coupled antennas," *IEEE Transactions on Antennas and Propagation*, vol. 56, no. 12, pp. 3650-3658, Dec. 2008.

[70] R. A. Bhatti, S. Yi, and S. Park, "Compact antenna array with port decoupling for LTE-standardized mobile phones," *IEEE Antennas and Wireless Propagation Letters*, vol. 8, pp. 1430-1433, 2009.

[71] A. C. K. Mak, C. R. Rowell, and R. D. Murch, "Isolation enhancement between two closely packed antennas," *IEEE Transactions on Antennas and Propagation*, vol.56, no.11, pp. 3411-3419, Nov. 2008.

[72] P. Ferrer, J. Arbesu, and J. Romeu, "Decorrelation of two closely spaced antennas with a metamaterial AMC surface," *Microwave and Optic. Tech. Lett.*, vol. 50, no. 5, May 2008.

[73] A. Abe, N. Michishita, Y. Yamada, J. Muramatsu, T. Watanabe, and K. Sato, "Mutual coupling reduction between two dipole antennas with parasitic elements composed of composite right-/left-handed transmission lines," *IEEE International Workshop on Antenna Technology (iWAT'2009)*, pp.1-4, Mar. 2009.

[74] C. Chi-Yuk, C. Chi-Ho, R. D. Murch, and C. R. Rowell, "Reduction of mutual coupling between closely-packed antenna elements," *IEEE Transactions on Antennas and Propagation*, vol. 55, no. 6, pp. 1732-1738, Jun. 2007.

[75] G. Yue, C. Xiaodong, Y. Zhinong, and C. Parini, "Design and performance investigation of a dual-element PIFA array at 2.5 GHz for MIMO terminal," *IEEE Transactions on Antennas and Propagation*, vol. 55, no. 12, pp. 3433-3441, Dec. 2007.

[76] C. Younkyu, J. Seong-Sik, D. Ahn, C. Jae-Ick, and T. Itoh, "High isolation dual-polarized patch antenna using integrated defected ground structure," *IEEE Microwave and Wireless Components Letters*, vol. 14, no. 1, pp. 4-6, Jan. 2004.

[77] H. Li, J. Xiong and S. He, "A compact planar MIMO antenna system of four elements with similar radiation characteristics and isolation structure," *IEEE Antennsa wireless propag. Lett.*, vol. 8, pp. 1107-1110, 2009.

[78] F. G. Zhu, J. D. Xu, and Q. Xu, "Reduction of mutual coupling between closely-packed antenna elements using defected ground structure," *Electronics Letters*, vol. 45, no. 12, pp. 601-602, Jun. 2009.

[79] A. Diallo, C. Luxey P. Le Thuc, R. Staraj, and G. Kossiavas, "Enhanced two-antenna structures for universal mobile telecommunications system diversity terminals," *IET Microwaves, Antennas & Propagation*, vol. 2, no. 1, pp. 93-101, Feb. 2008.

[80] A. Chebihi, C. Luxey, A. Diallo, P. Le Thuc, and R. Staraj, "A novel isolation technique for closely spaced PIFAs for UMTS mobile phones," *IEEE Antennas and Wireless Propagation Letters*, vol. 7, pp. 665-668, 2008.

[81] H. Minseok and C. Jaehoon, "Small-size printed strip MIMO antenna for next generation mobile handset application," *Microw. Opt. Technol. Lett.*, vol. 53, no. 2, pp. 48-352, 2011.

[82] I. Dioum, A. Diallo, C. Luxey, and S. M. Farsi, "Compact dual-band monopole antenna for LTE mobile phones," in Proceedings of the *Loughborough Antennas and Propagation Conference (LAPC)*, pp. 593-596, Nov. 2010.

[83] B. D. V. Veen and K. M. Buckley, "Beamforming: A versatile approach to spatial filtering," *IEEE ASSP Magazine*, vol. 5, no. 2, pp. 4-24, Apr. 1988.

[84] B. C. B. Peel, B. M. Hochwald and A. L. Swindlehurst, "A vector-perturbation technique for near-capacity multiantenna multiuser communication - Part I: channel inversion and regularization," *IEEE Trans. Commun.* vol. 53, no. 1, pp. 195-202, Jan. 2005.

[85] N. Jindal, "MIMO broadcast channels with finite rate feedback," *IEEE Trans. Information Theory.* vol. 52 no. 11, pp. 5045-5059, Nov. 2006.

[86] S. Stein, "On cross coupling in multiple -beam antennas," *IEEE Trans. Antennas Propag.*, vol. AP-10, no. 5, pp. 548557, Sep. 1962.

[87] http://www.dcsc.aau.dk/.

[88] B. Yanakiev, M. Christensen, and G. F. Pedersen, "MIMO OTA optical measurement device," *5th European Conf. Antennas and Propag. (EuCAP)*, pp. 58-61, 2011.